J. Phys. Earth, **32**, 511–529, 1984

SOURCE PARAMETERS RELEVANT TO HETEROGENEITY OF A FAULT PLANE

Yasuo IZUTANI

Department of Civil Engineering, Faculty of Engineering, Shinshu University, Nagano, Japan

(Received June 20, 1984; Revised November 30, 1984)

Accelerograms due to 16 earthquakes with JMA magnitude from 5.5 to 7.4 are analyzed. Second corner frequencies for the earthquakes are in a range from 1 to 8 Hz, and ratios of the rms stress-drop to the global stress-drop are from 2 to 10. The second corner frequency increases with the ratio of the rms stress-drop to the global stress-drop, and it is almost independent of the characteristic length of the fault plane. Based on stochastic source models, the second corner frequency is inversely proportional to an average size of element faults constituting a fault plane, so that the present result suggests that the average size decreases with increase in the heterogeneity of stress-drop on the fault plane. Also, the result implies that the average size of element faults is almost independent of the entire fault size for the earthquakes analyzed in this study.

1. *Introduction*

A deterministic source model such as HASKELL's (1964) can satisfactorily account for observed long-period seismic waves but not short-period seismic waves, because the faulting process of an actual earthquake is not so smooth as that assumed for the source model. The complexity of the faulting process plays an important role in radiating short-period seismic waves, and physical explanations of the radiation mechanism of short-period seismic waves have been presented by various stochastic source models which take heterogeneous characteristics of a fault plane into consideration (e.g., DAS and AKI, 1977; MIKUMO and MIYATAKE, 1978; HANKS, 1979; HIRASAWA, 1979; ANDREWS, 1981; PAPAGEORGIOU and AKI, 1981a, b; GUSEV, 1983; KOYAMA, 1983; SUZUKI and HIRASAWA, 1983).

In the meantime, several attempts have been made to clarify small-scale heterogeneities of fault planes of actual earthquakes. HIRASAWA (1979) assumed that an earthquake fault plane consists of a large number of element faults which are expressed by the crack model of SATO and HIRASAWA (1973). He showed that the spectral amplitude of high-frequency acceleration waves radiated from the fault plane is not controlled by an average value of stress-drops of the element faults but by the root-mean-square (rms) value of the stress-drops. Applying the method for estimating the maxima of a random function by CARTWRIGHT and LONGUET-HIGGINS (1956), he gave a relation between the rms stress-drop $\sqrt{\mathrm{E}\{\tau^2\}}$

and the maximum ground acceleration, then he estimated $\sqrt{E\{\tau^2\}}$'s for the Miyagi-Oki earthquakes of Feb. 20, 1978 and June 12, 1978 as 185 and 118 bar, respectively. These values are 2.6 and 1.7 times larger than global stress-drops of these earthquakes estimated from long-period data by SENO *et al.* (1980).

HANKS (1979) and HANKS and MCGUIRE (1981) presented an expression of the root-mean-square acceleration a_{rms} by applying BRUNE's (1970, 1971) source model. They estimated stress-drops from a_{rms} for 16 earthquakes and found that the stress-drops are very nearly equal to 100 bar for the earthquakes.

PAPAGEORGIOU and AKI (1981a, b) presented a specific barrier model. They assumed that an earthquake fault plane contains many small circular cracks surrounded by unbroken barriers. Applying the crack model of SATO and HIRASAWA (1973), they derived an expression of acceleration power spectra of S-waves. They analyzed 7 California earthquakes and found that the stress-drop at the element cracks, which is called local stress-drop $\Delta\sigma_1$, is a stable parameter ranging from 200 to 400 bar for all the earthquakes.

IZUTANI (1981, 1983) presented an expression of the source spectrum based on a hybrid of deterministic and stochastic source models. The source spectrum of acceleration has a frequency dependence of f^2—f^0—f^γ—f^0 from the low-frequency side. The frequency dependence with $\gamma=1$ is consistent with those of source spectra inferred from observed accelerograms due to earthquakes during the Matsushiro earthquake swarm from 1965 to 1970 (IZUTANI, 1981, 1983). It is also consistent with the frequency dependence of source spectra by AKI (1972) and with those numerically calculated by KOYAMA (1983) and SUZUKI and HIRASAWA (1983) based on stochastic source models. The frequency at the intersection of f^2 and f^0 trends is the corner frequency f_c and that at the intersection of f^1 and f^0 trends is the second corner frequency f_c^*. IZUTANI (1981, 1983) analyzed accelerograms of 14 Matsushiro earthquakes and 10 moderate to large size earthquakes near Japan, and found that the ratio of the rms stress-drop to the global stress-drop, $\sqrt{E\{\tau^2\}}/\Delta\sigma$, is in a range from 1 to 5.3. The second corner frequency f_c^* was found to increase with $\sqrt{E\{\tau^2\}}/\Delta\sigma$.

The stochastic source models have provided physical bases to prediction methods of the maximum acceleration by HIRASAWA (1979), the rms acceleration by HANKS (1979) and PAPAGEORGIOU and AKI (1981a, b), and realistic accelerograms by IZUTANI (1981, 1983) and SUZUKI and HIRASAWA (1983). However, knowledge of the heterogeneity of fault planes of actual earthquakes is too limited to give reliable bases to the methods. The attempt of the present study is to estimate the second corner frequency f_c^* and the ratio of the rms stress-drop to the global stress-drop, $\sqrt{E\{\tau^2\}}/\Delta\sigma$, through an analysis of accelerograms from earthquakes near Japan. Since the evaluation of the effect due to Q along the propagation path and amplification characteristics of soft surface layers at observation sites is difficult, we will analyze accelerograms recorded at four sites, Ofunato-bochi-S, Kushiro-S, Hachinohe-S, and Miyako-S, where conditions of

surface layers are relatively well known, due to earthquakes with source-to-site distances less than 100 km.

2. *Description of Earthquake Source Spectrum*

The source spectrum described here satisfies the source spectrum expected for the deterministic source model in a low-frequency range and that for HIRASAWA's (1979) stochastic source model in a high-frequency range. According to HIRASAWA (1979), the acceleration due to S-waves radiated from a large number of element faults constituting a circular fault of an earthquake can be approximated by a random pulse sequence. The length of the pulse sequence is about R/v_R, where R is the radius of the fault and v_R is the rupture velocity. When the pulses are observed at a distance r from the fault, the power spectral density of acceleration is given as,

$$S(\omega)=0.076\frac{v_S^3}{R}\frac{1}{\mu^2}\mathrm{E}\{\tau^2\}F(\alpha r, R/r)\,\mathrm{e}^{-2\alpha r}\,, \tag{1}$$

where v_S is the S-wave velocity, and μ is the rigidity. This is derived under an assumption that v_R is 75% of v_S. τ is the stress-drop at each small element fault and $\mathrm{E}\{\tau^2\}$ is the mean-square value of τ over the fault plane. $F(\alpha r, R/r)$ is a factor due to the difference in attenuation arising from the difference in distance between each of the element faults and the observation station, and it is nearly equal to $(R/r)^2$ when R/r is smaller than 1. α is defined as,

$$\alpha\equiv\pi f/v_S Q\,, \tag{2}$$

where f is the frequency and Q is the quality factor for S-waves along the wave propagation path. In (1), the radiation pattern of S-waves due to the focal mechanism of an earthquake is assumed to be 1.0, for simplicity. The Fourier spectral density of acceleration at a distance r in an infinite medium is expressed as,

$$\begin{aligned} A_S(f)&=\sqrt{2\pi S(\omega)R/v_R}\\ &=0.798\frac{v_S}{\mu}\sqrt{\mathrm{E}\{\tau^2\}F(\alpha r, R/r)}\,\mathrm{e}^{-\alpha r}\,, \end{aligned} \tag{3}$$

where v_R/v_S is again assumed to be 0.75.

In the meantime, the long-period spectral level Ω_0 of displacement spectrum expected for the deterministic source model is given as (HASKELL, 1964),

$$\Omega_0=\frac{M_0}{4\pi\rho r v_S^3}R_{\theta\phi}\,, \tag{4}$$

where $R_{\theta\phi}$ is the radiation pattern of S-waves, and M_0 is the seismic moment. In a circular crack model (BRUNE, 1970, 1971), M_0 is specifically expressed as,

$$M_0=\frac{16}{7}\Delta\sigma R^3\,, \tag{5}$$

where $\Delta\sigma$ is the global stress-drop on the fault plane. According to SATO and

HIRASAWA (1973), the expected value of the corner frequency f_c of S-wave spectrum is given as,

$$f_c=\frac{1.85\,v_S}{2\pi R}, \tag{6}$$

when $v_R/v_S=0.75$. Assuming ω^{-2} decay of the spectrum in a frequency range higher than f_c, the acceleration spectral density higher than f_c at a distance r is expressed as,

$$\begin{aligned} A_d(f)&=\Omega_0(2\pi f_c)^2\,e^{-\alpha r}\\ &=0.623\Delta\sigma\frac{v_S}{\mu}\frac{R}{r}e^{-\alpha r}, \end{aligned} \tag{7}$$

where $R_{\theta\phi}$ is assumed to be 1.0 as done in (1).

Since $\sqrt{F(\alpha r, R/r)}$ is nearly equal to R/r when R/r is smaller than 1, we replace R/r in (7) with $\sqrt{F(\alpha r, R/r)}$. Then, the ratio between the acceleration spectrum expected for the stochastic source model and that for the deterministic source model is approximately expressed as,

$$\frac{A_s(f)}{A_d(f)}=1.28\frac{\sqrt{E\{\tau^2\}}}{\Delta\sigma}. \tag{8}$$

The solid line in Fig. 1 schematically shows the source spectrum which

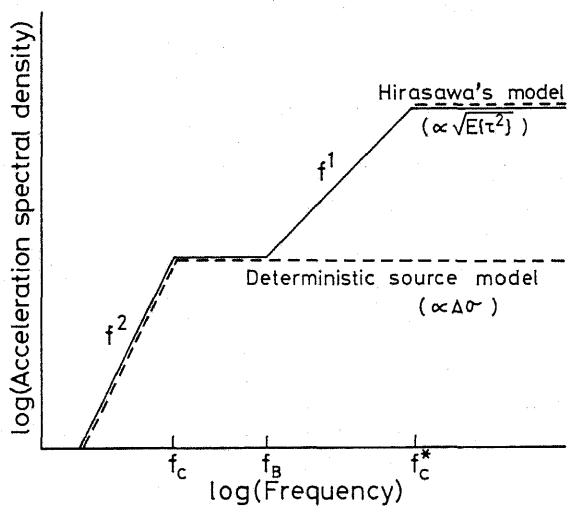

Fig. 1. Source spectra. The solid line indicates the source spectrum proposed in this study. The dashed lines are those expected for HIRASAWA's (1979) source model and for the deterministic source model. f_c is the corner frequency, and f_c^* is the second corner frequency. The proposed spectrum is larger than that for the deterministic source model in the frequency range higher than f_B. $\Delta\sigma$ and $\sqrt{E\{\tau^2\}}$ are the global stress-drop and the rms stress-drop, respectively, which are responsible for the spectral densities.

satisfies the source spectrum expected for HIRASAWA's (1979) model in the frequency range higher than the second corner frequency f_c^* and also satisfies that for the deterministic source model around and lower than the corner frequency f_c. In order to unite the source spectrum for Hirasawa's model and that for the deterministic source model smoothly, f^1 dependence of the spectrum is introduced in accordance with the results of previous studies (AKI, 1972; IZUTANI, 1981, 1983; KOYAMA, 1983; SUZUKI and HIRASAWA, 1983). The source spectrum is larger than that for the deterministic source model in a frequency range higher than f_B,

$$f_B=f_c^*/(1.28\sqrt{\mathrm{E}\{\tau^2\}}/\Delta\sigma)\,. \tag{9}$$

HANKS (1981) found the cut-off frequency f_{max} of observed acceleration spectra and concluded the cause of f_{max} as the effect of high-frequency attenuation through the propagation path and local surface layers. On the other hand, the existence of f_{max} in the source spectrum was pointed out by PAPAGEORGIOU and AKI (1981a, b) and YOKOI *et al.* (1983). However, since the evaluation of the effect due to Q is very difficult for high-frequency waves, it has not been clear whether or not f_{max} really exists in the source spectrum. Here, we assume that the source spectrum does not have f_{max} in the frequency range, from about 0.2 to about 13 Hz, of concern in this study.

3. *Method for Inference of Source Parameters from Accelerograms*

We attempt to estimate source parameters relevant to heterogeneity of a fault plane from the total power E_i of band-pass filtered ground acceleration. E_i is one of the most useful parameters to express characteristics of ground acceleration (IZUTANI, 1981, 1983), and it is calculated from the ground acceleration $x(t)$ as,

$$E_i=\int_0^{T_d}[\{x(t)\cdot W(t)\}*h_i(t)]^2\,\mathrm{d}t\,, \tag{10}$$

where T_d is the full record length. A window function,

$$W(t)=\begin{cases}1; & t_1\leqq t\leqq t_2\,,\\ 0; & \text{otherwise}\,,\end{cases} \tag{11}$$

where t_1 and t_2-t_1 are the arrival time and the duration of S-waves, respectively, is multiplied to $x(t)$ for isolating the ground acceleration due to S-waves. The band-pass filter $h_i(t)$ is assumed to be similar to the velocity response of an oscillator with one-degree-of-freedom to the input acceleration, and the impulse response is given as,

$$\begin{aligned}h_i(t)&=4\pi\beta f_i\{\cos\omega_d t-\beta_d\sin\omega_d t\}\,\mathrm{e}^{-2\pi\beta f_i t}\,,\\ &\begin{cases}\omega_d=2\pi f_i\sqrt{1-\beta^2}\,,\\ \beta_d=\beta/\sqrt{1-\beta^2}\,,\end{cases}\end{aligned} \tag{12}$$

where f_i and β are the central frequency of the i-th filter and the damping coefficient of the oscillator, respectively. Considering the frequency band-width of the filter, β is assumed to be 0.1 and f_i is so chosen as to be equally spaced on the logarithmic scale. We limit f_i in a frequency range from $\log f_1=-0.64$ ($f_1\simeq 0.23$ Hz) to $\log f_{12}=1.12$ ($f_{12}\simeq 13$ Hz) in consideration of the frequency characteristics of the SMAC-B2 accelerograph whose records will be analyzed later.

Theoretically, an expression of E_i in the frequency range higher than f_c^* is derived from the source spectrum $A_s(f)$ in (3) as,

$$E_i=\frac{1}{2}\{cA_s(f)G_i\}^2\left\{2\int_0^\infty |H_i(f)|^2 df\right\}, \tag{13}$$

where

$$G_i=\left[\left\{\int_0^\infty |G(f)H_i(f)|^2 df\right\}\Big/\left\{\int_0^\infty |H_i(f)|^2 df\right\}\right]^{1/2}. \tag{14}$$

$G(f)$ is the amplification characteristics of surface layers at an observation site, and $H_i(f)$ is the frequency characteristics of the i-th band-pass filter. c is a coefficient to take into account the difference between the medium in the source region and that in the basement rock under an observation site, and is approximated as,

$$c=\sqrt{\rho v_S/\rho_0 v_{S_0}}, \tag{15}$$

where ρ and v_S are the density and the S-wave velocity in the source region, and ρ_0 and v_{S_0} are those in the basement rock. The factor 1/2 in (13) is for the vectorial partition of the wave energy into two horizontal components with an equal amplitude. Approximating the characteristics of the filter as,

$$2\int_0^\infty |H_i(f)|^2 df\simeq 0.63 f_i, \tag{16}$$

and putting (3) into (13), the theoretical expression of E_i for $f_i\geqq f_c^*$ is reduced to,

$$E_i=0.20\frac{c^2}{\rho^2 v_S{}^2}\mathrm{E}\{\tau^2\}F(\alpha_i r, R/r)G_i^2 f_i e^{-2\alpha_i r}; \qquad f_i\geqq f_c^*, \tag{17}$$

where

$$\alpha_i=\pi f_i/v_S Q. \tag{18}$$

Considering the spectral structure in Fig. 1 and the spectral ratio in (8), theoretical expressions of E_i in the other frequency range are given as,

$$E_i=\begin{cases} 0.20\dfrac{c^2}{\rho^2 v_S{}^2}\mathrm{E}\{\tau^2\}F(\alpha_i r, R/r)G_i^2 f_i\left(\dfrac{f_i}{f_c^*}\right)^2 e^{-2\alpha_i r}; & f_B\leqq f_i<f_c^*, \\ 0.20\dfrac{c^2}{\rho^2 v_S{}^2}\left(\dfrac{\Delta\sigma}{1.28}\right)^2 F(\alpha_i r, R/r)G_i^2 f_i e^{-2\alpha_i r}; & f_c\leqq f_i<f_B, \\ 0.20\dfrac{c^2}{\rho^2 v_S{}^2}\left(\dfrac{\Delta\sigma}{1.28}\right)^2 F(\alpha_i r, R/r)G_i^2 f_i\left(\dfrac{f_i}{f_c}\right)^4 e^{-2\alpha_i r}; & f_i<f_c. \end{cases} \tag{19}$$

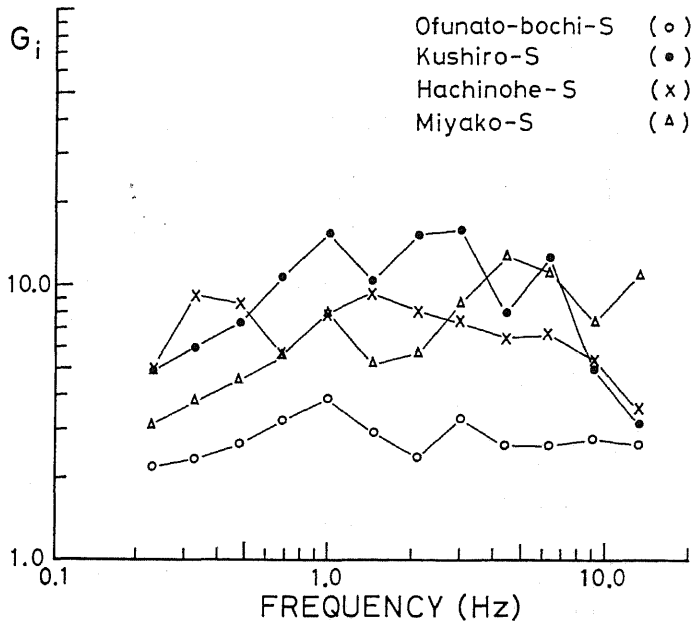

Fig. 2. Amplification characteristics G_i of surface layers at each observation site.

The second corner frequency f_c^*, the global stress-drop $\Delta\sigma$, and the rms stress-drop $\sqrt{\mathrm{E}\{\tau^2\}}$ are estimated by minimizing the sum of squares of residuals between $\log E_i$ (i=1–12) inferred from an acceleration record by (10) and that theoretically calculated by (17) and (19). For the theoretical calculation of $\log E_i$, the amplification characteristics of surface layers at observation sites are approximated by those due to the vertical incidence of plane SH-waves from the basement rock, for simplicity. We use KOBAYASHI and KAGAMI's (1966) method and layer parameters estimated by MIDORIKAWA and KOBAYASHI (1978) and HIRASAWA (1980) to calculate G_i's shown in Fig. 2. The average value of the quality factor Q along the propagation path is assumed to be 200 in the frequency range lower than 1 Hz and $200\sqrt{f}$ in the frequency range higher than 1 Hz with reference to GUSEV (1983) and YOKOI *et al.* (1983). The S-wave velocity and the density in the source region are assumed to be 3.5 km/s and 3.0 g/cm^3, respectively. The characteristic length L of a fault plane is estimated as a fault diameter of an equivalent circular fault for earthquakes of which fault areas have been estimated by previous studies. For the other earthquakes, L is estimated from the earthquake magnitude by using OTSUKA's (1964) empirical formula,

$$\log L = 0.5M - 1.8 \,. \tag{20}$$

4. *Analysis and Result*

The data to be analyzed are composed of 32 digital accelerograms of hori-

Table 1. Data.

Record No.	Date (Year Month Day)	M	h (km)	L (km)	r (km)
(Observed at Ofunato-bochi-S)					
S- 554	1970. 9. 14	6.2	40	20	65
S- 786	1973. 11. 19	6.4	50	25	50
S-1022	1977. 6. 8	5.8	70	13	86
S-1210	1978. 6. 12	7.4	40	55	82
S-1494	1982. 6. 1	6.2	40	20	65
(Observed at Kushiro-S)					
S- 369	1968. 8. 17	5.7	80	11	87
S- 674	1972. 5. 11	5.8	60	13	80
S- 858	1974. 9. 20	5.5	50	9	79
(Observed at Hachinohe-S)					
S- 469	1969. 6. 21	5.6	40	10	81
S- 857	1974. 9. 4	5.6	40	10	64
S-1168	1978. 5. 16	5.8	10	13	40
S-1169	1978. 5. 16	5.8	10	13	38
(Observed at Miyako-S)					
S- 273	1968. 5. 23	6.3	30	10	86
S- 312	1968. 6. 12	7.2	0	55	75
S- 420	1968. 11. 14	6.0	30	16	87
S- 537	1970. 4. 1	5.8	80	13	74

M, JMA magnitude; h, focal depth; L, fault diameter; r, source-to-site distance.
L's for S-1210, S-273, and S-312 are evaluated from fault areas estimated by SENO *et al.* (1980), IZUTANI and HIRASAWA (1978), and YOSHIOKA and ABE (1976), respectively. The other values of L are evaluated by the empirical relation (20).

zontal components from 16 earthquakes as shown in Table 1. All the accelerograms have been digitized and published by the Port and Harbour Research Institute (KURATA *et al.*, 1973, 1974, 1975, 1978, 1979, 1980, 1983; TSUCHIDA *et al.*, 1970a, b, 1971). These accelerograms are chosen through the following criteria; (i) the source-to-site distance is smaller than 100 km so that the attenuation and scattering effects are small, (ii) the condition of surface layers at the observation site is well known so that the amplification characteristics can be estimated reliably. The accelerograms are those due to earthquakes near Japan with JMA magnitudes ranging from 5.5 to 7.4. The maximum accelerations range from 41 to 287 gal. The correction of instrumental response is carried out in the frequency domain with the theoretical response characteristics of SMAC-B2 type accelerograph.

The Husid-plot,

$$P(t)=\left(\int_0^t \{x(t')\}^2 dt'\right)\Big/\left(\int_0^{T_d} \{x(t')\}^2 dt'\right), \tag{21}$$

is calculated for determining the length of the S-wave arrival window $W(t)$ in (11). Figure 3 shows ground accelerations of two horizontal components and Husid-

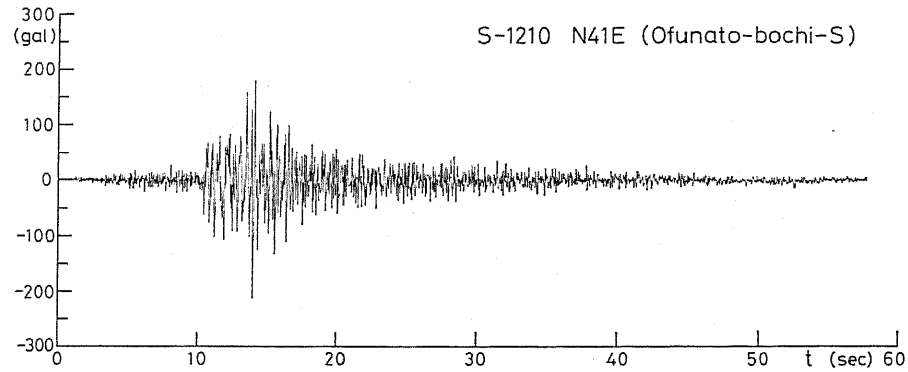

(a)

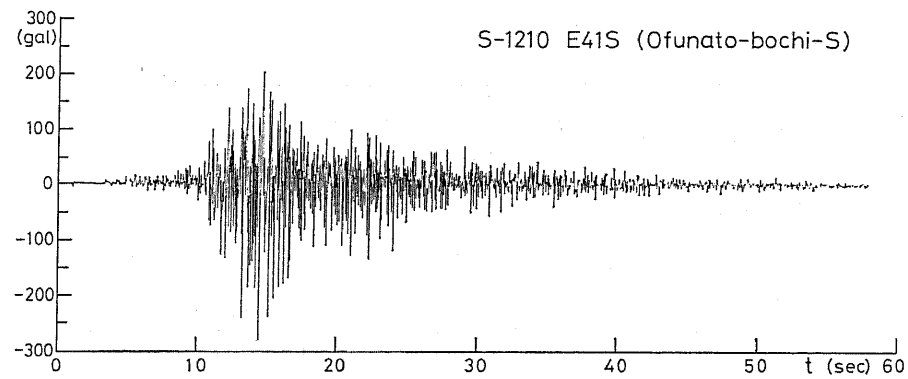

(b)

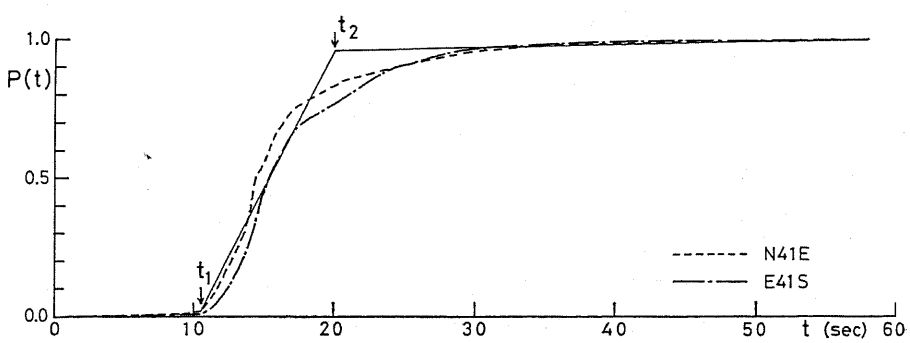

(c)

Fig. 3. Ground accelerations and Husid-plots for the record S-1210. The solid lines show approximate trends of the Husid-plots. The acceleration records between t_1 and t_2 are regarded as those due to S-waves.

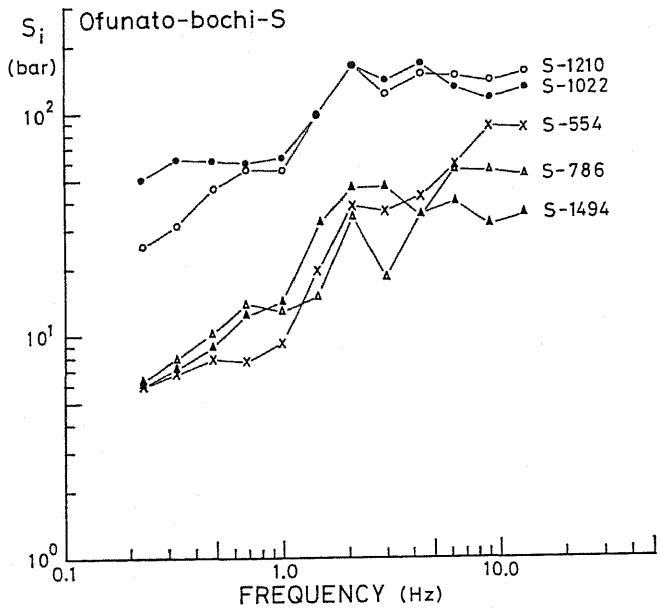

Fig. 4(a)

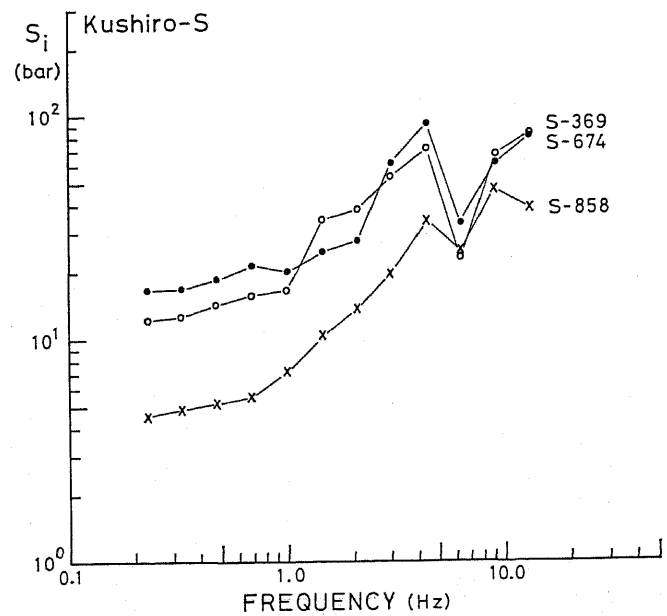

Fig. 4(b)

Fig. 4. (a) Source spectral structures for the records observed at Ofunato-bochi-S. (b) Source spectral structures for the records observed at Kushiro-S. (c) Source spectral structures for the records observed at Hachinohe-S. (d) Source spectral structures for the records observed at Miyako-S.

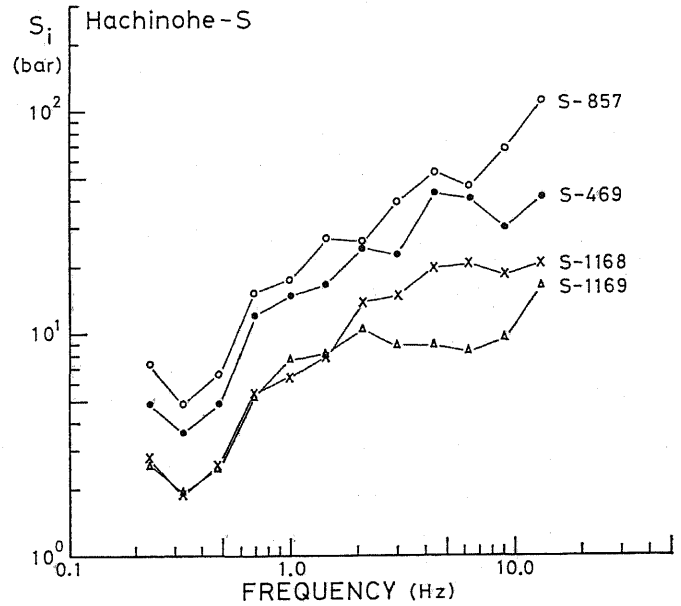
Hachinohe-S
S_i
(bar)
10^2
10^1
10^0
0.1
1.0
10.0
FREQUENCY (Hz)
S-857
S-469
S-1168
S-1169

Fig. 4(c)

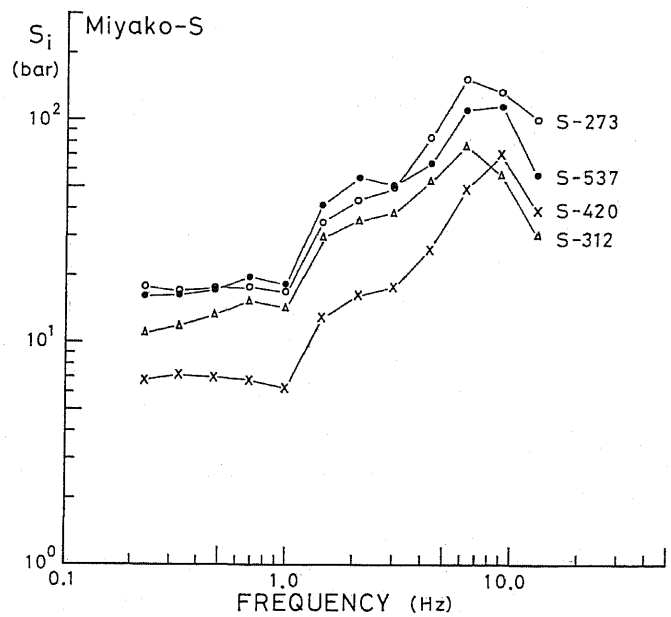
Miyako-S
S_i
(bar)
10^2
10^1
10^0
0.1
1.0
10.0
FREQUENCY (Hz)
S-273
S-537
S-420
S-312

Fig. 4(d)

plots for the record S-1210. We can easily point out the S-wave arrival time t_1 but not the end time t_2 in the ground acceleration records. According to DOBRY *et al.* (1978) and IZUTANI (1983), a portion with relatively high-rate increase in the Husid-plot is mainly due to S-waves. Therefore, we point out the time t_2 approximately at the intersection of two line segments along the portion with high-rate increase in $P(t)$ and that with low-rate increase in $P(t)$ due to later arrival waves as shown in Fig. 3.

Total powers of band-pass filtered ground accelerations of two horizontal components at the same observation site for the same earthquake generally differ from each other, and the differences sometimes amount to a factor of 3 or 4. This may be mainly because of the effect of the focal mechanism of the earthquake with respect to the orientation of the instruments. However, since the averaged nature of this effect is only taken into account in the present study, E_i is obtained as an average of E_i's of the two horizontal components of ground acceleration.

The source spectral structure,

$$S_i=\begin{cases}\sqrt{\mathrm{E}\{\tau^2\}}; & f_c^*\leqq f_i\,,\\ \sqrt{\mathrm{E}\{\tau^2\}}\dfrac{f_i}{f_c^*}; & f_B\leqq f_i<f_c^*\,,\\ \dfrac{\Delta\sigma}{1.28}; & f_c\leqq f_i<f_B\,,\\ \dfrac{\Delta\sigma}{1.28}\left(\dfrac{f_i}{f_c}\right)^2; & f_i<f_c\,,\end{cases} \tag{22}$$

is derived from E_i of observed ground acceleration by subtracting the effects of the other terms in the theoretical expressions of E_i in (17) and (19). Thus obtained, S_i in Fig. 4(a) through (d) can be directly compared with the theoretical source spectrum in Fig. 1.

Since corner frequencies evaluated by (6) are lower than 0.2 Hz for these earthquakes, spectral corners appearing in the frequency range from 1 to 10 Hz in Fig. 4(a) through (d) are different from the corner frequencies. In the meantime, global stress-drops of the earthquakes corresponding to the records, S-1210, S-273, and S-312, have been estimated as 70, 23, and 12 bar from long-period data by SENO *et al.* (1980), IZUTANI and HIRASAWA (1978), and YOSHIOKA and ABE (1976), respectively. The rms stress-drops for these earthquakes, which are estimated from the high-frequency spectral level of S_i's, are much larger than the global stress-drops.

A systematic difference in spectral structure is seen among data for different observation sites. Probably, the main cause of the systematic difference is that the compensation of the effect of surface layers with the theoretical amplification characteristics G_i is not perfect. For example, troughs at about 6 Hz in S_i's in Fig. 4(b) correspond to a peak in G_i for Kushiro-S. Also, the sudden decrease in S_i's at about 13 Hz in Fig. 4(d) corresponds to the sudden increase in G_i for

Miyako-S. The systematic difference would affect absolute values of the second corner frequency f_c^*, the global stress-drop $\Delta\sigma$, and the rms stress-drop $\sqrt{\overline{E\{\tau^2\}}}$, which will be estimated later, but it would not so strongly affect the relative values of the parameters among earthquakes at the same observation site.

The spectral structure S_i for S-1210 and that for S-1494 in Fig. 4(a) resemble each other in spite of the difference in earthquake magnitude. This fact suggests that heterogeneities of the fault planes of these earthquakes are almost the same independently of the fault plane size. Meanwhile, S_i for S-554 and that for S-1494 in Fig. 4(a) almost agree with each other in the frequency range lower than about 3 Hz, but they are different from each other in the higher frequency range. Although the magnitudes of these earthquakes are the same, heterogeneities of the fault planes may be different from each other. A similar phenomenon is seen in S_i's for S-1168 and S-1169 in Fig. 4(c).

The global stress-drop $\Delta\sigma$, the rms stress-drop $\sqrt{\overline{E\{\tau^2\}}}$ and the second corner frequency f_c^* are estimated by the method described in Sec. 3, and the result is tabulated in Table 2. As mentioned above, the values of $\Delta\sigma$ obtained by other authors are 70, 23, and 12 bar for S-1210, S-273, and S-312, respectively. These values are somewhat different from corresponding values in Table 2. Not only $\Delta\sigma$ but also $\sqrt{\overline{E\{\tau^2\}}}$ in Table 2 might contain some error, because they are estimated based upon various assumptions on the radiation pattern, the rupture velocity, the characteristic length of a fault plane, the attenuation factor, and amplification

Table 2. Source parameters.

Record No.	$\Delta\sigma$ (bar)	$\sqrt{\overline{E\{\tau^2\}}}$ (bar)	f_c^* (Hz)
(Observed at Ofunato-bochi-S)			
S- 554	9	87	7.5
S- 786	12	55	5.5
S-1022	74	137	2.0
S-1210	35	145	2.0
S-1494	7	38	2.0
(Observed at Kushiro-S)			
S- 369	16	55	2.8
S- 674	24	62	3.7
S- 858	6	35	5.0
(Observed at Hachinohe-S)			
S- 469	5	34	2.7
S- 857	7	70	4.7
S-1168	3	20	3.3
S-1169	3	10	1.5
(Observed at Miyako-S)			
S- 273	22	123	6.3
S- 312	16	50	3.2
S- 420	9	52	7.4
S- 537	22	83	3.8

$\Delta\sigma$, global stress-drop; $\sqrt{\overline{E\{\tau^2\}}}$, rms stress-drop; f_c^*, second corner frequency.

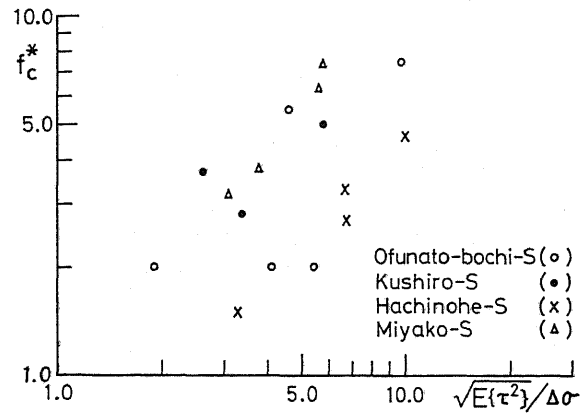

Fig. 5. Relation between f_c^* and $\sqrt{E\{\tau^2\}}/\Delta\sigma$. f_c^* is the second corner frequency, and $\sqrt{E\{\tau^2\}}/\Delta\sigma$ is the ratio of the rms stress-drop to the global stress-drop. Data for different observation sites are plotted by different symbols.

characteristics of surface layers at observation sites. The error in f_c^* due to the systematic difference in spectral structure among data for different sites might be at most several tens of percent. To avoid influence due to the assumptions, we will discuss relative values among f_c^*'s and those among $\sqrt{E\{\tau^2\}}/\Delta\sigma$'s for earthquakes observed at the same site.

Figure 5 shows the relation between f_c^* and $\sqrt{E\{\tau^2\}}/\Delta\sigma$. Data at different observation sites are plotted using different symbols. A linear correlation between $\log f_c^*$ and $\log(\sqrt{E\{\tau^2\}}/\Delta\sigma)$ is seen in Fig. 5. We carry out a regression analysis of $\log f_c^*$ in terms of $\log(\sqrt{E\{\tau^2\}}/\Delta\sigma)$, $\log L$, and dummy variables x_j ($j=1$–3) which are introduced to take the difference in observation site into account. (x_1, x_2, x_3) is equal to (0, 0, 0) for data at Ofunato-bochi-S, (1, 0, 0) at Kushiro-S, (0, 1, 0) at Hachinohe-S, and (0, 0, 1) at Miyako-S. The result of the regression analysis is as follows:

$$\log f_c^* = b_0 + b_1 \log(\sqrt{E\{\tau^2\}}/\Delta\sigma) + b_2 \log L + \sum_{j=1}^{3} c_j x_j , \tag{23}$$

$$\begin{cases} b_0 = 0.23 , \\ b_1 = 0.79 , \\ b_2 = -0.18 , \end{cases} \qquad \begin{cases} c_1 = 0.07 , \\ c_2 = -0.22 , \\ c_3 = 0.17 . \end{cases}$$

The multiple regression coefficient is 0.83. The 90 percent confidence ranges for the parameters b_1 and b_2 are from 0.41 to 1.17 and from -0.53 to 0.18, respectively.

According to KOYAMA (1983) and SUZUKI and HIRASAWA (1983) the second corner frequency f_c^* is inversely proportional to an average size $E\{\Delta L\}$ of element faults. In the meantime, the ratio of the rms stress-drop to the global stress-drop, $\sqrt{E\{\tau^2\}}/\Delta\sigma$, expresses the extremeness of the heterogeneity of a fault plane. Therefore, the present result suggests that $E\{\Delta L\}$ decreases with increase in the hetero-

geneity and that $E\{\Delta L\}$ is almost independent of the characteristic length L of the fault plane.

5. *Discussion*

It has been pointed out by various investigators, as described in Sec. 1, that "actual" stress-drop relevant to the radiation of high-frequency waves is much larger than the global stress-drop estimated from long-period data. The ratios of the rms stress-drop $\sqrt{E\{\tau^2\}}$ to the global stress-drop $\Delta\sigma$ estimated in the present study range from about 2 to 10. Although results by different investigators cannot be directly compared because of the difference in data and also because of the difference in assumptions on the rupture velocity, the quality factor, the site condition, and so on, the present result is consistent with the results of the previous studies in that the actual stress-drop is larger than the global stress-drop.

The present result (23) is reduced to

$$f_c^*=1.7\left(\frac{\sqrt{E\{\tau^2\}}}{\Delta\sigma}\right)^{0.8}\left(\frac{1}{L}\right)^{0.2}. \tag{24}$$

The constant in (24) is that for records at Ofunato-bochi-S where the instruments are installed on hard rock. This relation gives a set of source spectra for constant $\Delta\sigma$. Figure 6 shows source spectra for the cases of $L=10$ and 100 km, and $\sqrt{E\{\tau^2\}}/\Delta\sigma=2$ and 5. The long-period parts of the spectra are given by the deterministic source model. The second corner frequency f_c^* is clearly different from the corner frequency f_c expected from the deterministic source model, and f_c^*/f_c is not constant. The difference in $\sqrt{E\{\sigma^2\}}/\Delta\sigma$ has an effect only on the spectra in the frequency range higher than f_c^*, and f_B is almost independent of $\sqrt{E\{\tau^2\}}/\Delta\sigma$.

UMEDA (1981) found that the second corner frequency in P-wave spectra is almost independent of the earthquake magnitude. Relations of the second corner frequency f_c^* in S-wave spectra to the source size have been obtained by IZUTANI (1983) for moderate to large earthquakes near Japan, and by IRIKURA and YOKOI (1984) for aftershocks of the Nihonkai-Chubu earthquake of 1983. These relations and the present result are consistent with that of UMEDA (1981). On the other hand, KOYAMA (1983) and IZUTANI (1983) pointed out that f_c^*'s for Matsushiro earthquakes, which are shallow strike-slip ones with JMA magnitudes from 4.2 to 5.1, appear to have a proportionality to $M_0^{1/3}$ or to L^{-1}. This is similar to the well-known relation between the corner frequency f_c and M_0. There might be a regional variation in the relation between f_c^* and the source size.

Now, we discuss the physical background of the present result in connection with stochastic source models. PAPAGEORGIOU and AKI's (1981a, b) specific barrier model and HIRASAWA's (1979) patch model are opposite extreme cases of stochastic source models. In the specific barrier model, since the element cracks surrounded by unbroken barriers are assumed to have the same size and the same amount of slippage, the relation among the average stress-drop $E\{\tau\}$, the rms stress-drop

$\sqrt{\mathrm{E}\{\tau^2\}}$, the global stress-drop $\Delta\sigma$, and the local stress-drop $\Delta\sigma_1$ is

$$\Delta\sigma \leqq \Delta\sigma_1 = \mathrm{E}\{\tau\} = \sqrt{\mathrm{E}\{\tau^2\}}\,. \tag{25}$$

The size of element cracks in the specific barrier model corresponds to the average size $\mathrm{E}\{\Delta L\}$ of element faults, so that a relation,

$$\frac{L}{\mathrm{E}\{\Delta L\}} \simeq \frac{\Delta\sigma_1}{\Delta\sigma}\,, \tag{26}$$

is expected for the model. According to KOYAMA (1983) and SUZUKI and HIRASAWA (1983), f_c^* is inversely proportional to $\mathrm{E}\{\Delta L\}$. Therefore, the specific barrier model can explain the positive correlation between f_c^* and $\sqrt{\mathrm{E}\{\tau^2\}}/\Delta\sigma$, and the relation between f_c^* and L for the Matsushiro earthquakes, but the relation between f_c^* and L for earthquakes near Japan is not consistent with the model.

On the other hand, since the patch model has no barrier on a fault plane, the relation among $\mathrm{E}\{\tau\}$, $\sqrt{\mathrm{E}\{\tau^2\}}$, and $\Delta\sigma$ is

$$\Delta\sigma = \mathrm{E}\{\tau\} \leqq \sqrt{\mathrm{E}\{\tau^2\}}\,. \tag{27}$$

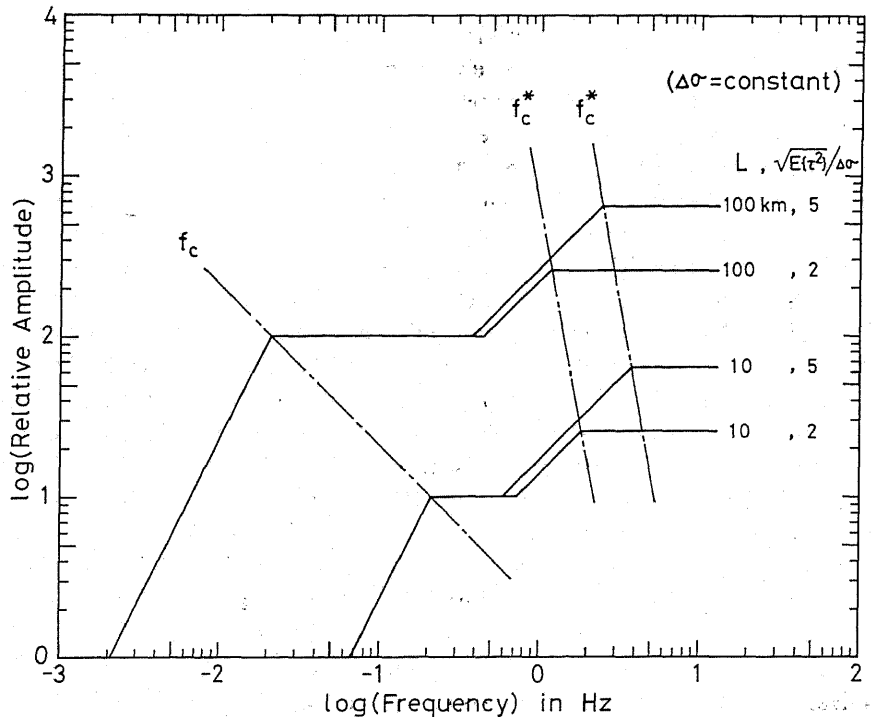

Fig. 6. Acceleration source spectra expected from the present result. The global stress-drop $\Delta\sigma$ is assumed to be constant. f_c and f_c^* are the corner frequency and the second corner frequency, respectively. L is the characteristic length of a fault plane, and $\sqrt{\mathrm{E}\{\tau^2\}}/\Delta\sigma$ is the ratio of the rms stress-drop to the global stress-drop.

In this model, the size of element faults is independent of $E\{\tau\}$, $\sqrt{E\{\tau^2\}}$, or L, so that the present result that $E\{\Delta L\}$ is almost independent of L is consistent with the patch model. However, since $E\{\tau\}$ should be equal to $\Delta\sigma$ as in (27), it is necessary to consider a relatively small number of asperities which have extremely large strength in comparison with the rest of the fault plane in order to explain a large value of $\sqrt{E\{\tau^2\}}/\Delta\sigma$, for example 10. Gaussian distribution or Weibull's distribution cannot explain $\sqrt{E\{\tau^2\}}/\Delta\sigma=10$, and so the present result requires a bi-modal or a more complex distribution of stress-drop on the fault plane. Also, the positive correlation between f_c^* and $\sqrt{E\{\tau^2\}}/\Delta\sigma$ requires that the fracture strength of asperities relative to the rest of the fault plane is larger for smaller asperities.

It may be natural to consider a hybrid model of barrier and patch models (AKI, 1983; IZUTANI, 1983). A fault plane is assumed to be divided into a few fault segments by barriers, and asperities are assumed to be included in each fault segment. Since the average stress-drop $E\{\tau\}$ on each fault segment is larger than $\Delta\sigma$ as expected from the barrier model, $\sqrt{E\{\tau^2\}}/E\{\tau\}$ on each fault segment is not so large as $\sqrt{E\{\tau^2\}}/\Delta\sigma$. Therefore, we need not consider extreme distributions for the stress-drop and the size of element faults on a fault plane in order to explain the observational results.

As AKI (1983) stated, the ultimate goal of strong motion seismology is the prediction of strong ground motion for future earthquakes. Attempts have been made to apply stochastic source models for predicting strong ground motion (e.g., HANKS, 1979; HIRASAWA, 1979; IZUTANI, 1981, 1983; PAPAGEORGIOU and AKI, 1981a, b; SUZUKI and HIRASAWA, 1983). The present results provide useful knowledge for the prediction methods. However, more detailed knowledge of the heterogeneity is required to use the methods for the practical purpose of earthquake resistant design. It is necessary to study characteristics of source parameters relevant to the heterogeneity of a fault plane by analyzing more accelerograms from earthquakes of various size in various regions.

6. *Conclusion*

Characteristics of source parameters relevant to the heterogeneity of a fault plane have been studied through the analysis of accelerograms from 16 earthquakes near Japan. The results obtained can be summarized as follows:

1) The second corner frequency f_c^* is found in a frequency range from 1 to 8 Hz.

2) The ratio of the rms stress-drop to the global stress-drop, $\sqrt{E\{\tau^2\}}/\Delta\sigma$, ranges from 2 to 10.

3) The second corner frequency f_c^* increases with $\sqrt{E\{\tau^2\}}/\Delta\sigma$, and it is almost independent of the characteristic length of the fault plane.

Based on stochastic source models, the present results suggest that the average size of element faults decreases with increase in the heterogeneity of stress-drop on the fault plane. Also, the results imply that the average size of element faults

is almost independent of the entire fault size for the earthquakes analyzed in this study.

The author wishes to express his sincere gratitude to Prof. Z. Suzuki, Prof. A. Takagi, Prof. T. Hirasawa, and Prof. H. Sima for their kind guidance and encouragement. Critical comments by Prof. K. Aki, Drs. J. Koyama, T. C. Hanks, and A. A. Gusev are much appreciated. Drs. H. Tsuchida, S. Noda, E. Kurata, and S. Iai of the Port and Harbour Research Institute, Ministry of Transport, are also acknowledged for allowing the use of magnetic tapes of digital accelerograms. HITAC M-240H computer of the Computer Center of Shinshu University was used for processing data.

REFERENCES

AKI, K., Scaling law of earthquake source time-function, *Geophys. J. R. Astron. Soc.*, **31**, 3–25, 1972.

AKI, K., Strong motion seismology, in *Earthquakes: Observation, Theory and Interpretation*, ed. H. Kanamori and E. Boschi, pp. 223–250, Soc. Italiana di Fisica, Bologna, Italy, 1983.

ANDREWS, D. J., A stochastic fault model 2. Time-dependent case, *J. Geophys. Res.*, **86**, 10821–10834, 1981.

BRUNE, J. N., Tectonic stress and spectra of seismic shear waves from earthquakes, *J. Geophys. Res.*, **75**, 4997–5009, 1970.

BRUNE, J. N., Correction, *J. Geophys. Res.*, **76**, 5002, 1971.

CARTWRIGHT, D. E. and M. S. LONGUET-HIGGINS, The statistical distribution of the maxima of a random function, *Proc. R. Soc. London, Ser. A*, **237**, 212–232, 1956.

DAS, S. and K. AKI, Fault plane with barriers: A versatile earthquake model, *J. Geophys. Res.*, **82**, 5658–5670, 1977.

DOBRY, R., I. M. IDRISS, and E. NG, Duration characteristics of horizontal components of strong-motion earthquake records, *Bull. Seismol. Soc. Am.*, **68**, 1487–1520, 1978.

GUSEV, A. A., Descriptive statistical model of earthquake source radiation and its application to an estimate of short-period strong motion, *Geophys. J. R. Astron. Soc.*, **74**, 787–808, 1983.

HANKS, T. C., b values and $\omega^{-\gamma}$ seismic source models: Implications for tectonic stress variations along active crustal fault zones and the estimation of high-frequency strong ground motion, *J. Geophys. Res.*, **84**, 2235–2242, 1979.

HANKS, T. C., f_{max}, Proc. USGS Workshop XVI, 405–436, 1981.

HANKS, T. C. and R. K. MCGUIRE, The character of high-frequency strong ground motion, *Bull. Seismol. Soc. Am.*, **71**, 2071–2095, 1981.

HASKELL, N. A., Total energy and energy spectral density of elastic wave radiation from propagating faults, *Bull. Seismol. Soc. Am.*, **54**, 1811–1841, 1964.

HIRASAWA, T., Prediction of maximum acceleration due to a stochastic source model, Rep. Special Research on National Disasters, No. A-54-3, 35–45, 1979 (in Japanese).

HIRASAWA, T., Seismic activity, in *General Report on the 1978 Miyagi-Oki Earthquake*, pp. 7–28, Tohoku Branch of Japan Soc. Civil Eng., 1980 (in Japanese).

IRIKURA, K. and T. YOKOI, Scaling law of acceleration spectra, Abst. Meet. Seismol. Soc. Japan, No. 1, C20, 1984 (in Japanese).

IZUTANI, Y., A statistical model for prediction of quasi-realistic strong ground motion, *J. Phys. Earth*, **29**, 537–557, 1981.

IZUTANI, Y., Analysis of accelerograms and prediction of strong ground motion based on a stochastic source model, Doctoral thesis, Tohoku Univ., 1983.

IZUTANI, Y. and T. HIRASAWA, Source characteristics of shallow earthquakes in the northern part of Sanriku-Oki region, Japan, *J. Phys. Earth*, **26**, 275–297, 1978.

KOBAYASHI, H. and H. KAGAMI, Numerical method for analyzing earthquake response of stratified layers by use of the ray theory, Proc. 2nd Japan Earthq. Eng. Symp., 15–19, 1966 (in Japanese).

KOYAMA, J., Earthquake source spectrum from coherent and incoherent rupture on a fault, *Zisin, Ser. 2*, **36**, 225–235, 1983 (in Japanese with English abstract).

KURATA, E., T. FUKUHARA, and S. NODA, Annual report on strong-motion earthquake records in Japanese ports (1982), *Tech. Note Port Harbour Res. Inst.*, No. 446, 1983.

KURATA, E., S. IAI, and H. TSUCHIDA, Annual report on strong-motion earthquake records in Japanese ports (1976 and 1977), *Tech. Note Port Harbour Res. Inst.*, No. 287, 1978.

KURATA, E., T. ISHIZAKA, and H. TSUCHIDA, Annual report on strong-motion earthquake records in Japanese ports (1972), *Tech. Note Port Harbour Res. Inst.*, No. 160, 1973.

KURATA, E., T. ISHIZAKA, and H. TSUCHIDA, Annual report on strong-motion earthquake records in Japanese ports (1973), *Tech. Note Port Harbour Res. Inst.*, No. 181, 1974.

KURATA, E., T. ISHIZAKA, and H. TSUCHIDA, Annual report on strong-motion earthquake records in Japanese ports (1974), *Tech. Note Port Harbour Res. Inst.*, No. 202, 1975.

KURATA, E., S. IAI, Y. YOKOYAMA, and H. TSUCHIDA, Strong-motion earthquake records on the 1978 Miyagi-Ken-Oki earthquake in port areas, *Tech. Note Port Harbour Res. Inst.*, No. 319, 1979.

KURATA, E., S. IAI, Y. YOKOYAMA, and H. TSUCHIDA, Annual report on strong-motion earthquake records in Japanese ports (1978 and 1979), *Tech. Note Port Harbour Res. Inst.*, No. 338, 1980.

MIDORIKAWA, S. and H. KOBAYASHI, Spectral characteristics of incident wave from seismic bedrock due to earthquake, *Trans. Arch. Inst. Jpn.*, No. 273, 43–54, 1978 (in Japanese with English summary).

MIKUMO, T. and T. MIYATAKE, Dynamical rupture process on a three-dimensional fault with non-uniform frictions and near-field seismic waves, *Geophys. J. R. Astron. Soc.*, **54**, 417–438, 1978.

OTSUKA, M., Earthquake magnitude and surface fault formulation, *J. Phys. Earth*, **12**, 19–24, 1964.

PAPAGEORGIOU, A. S. and K. AKI, A specific barrier model for the quantitative description of inhomogeneous faulting and the prediction of strong ground motion I. Description of the model, Proc. USGS Workshop XVI, 331–352, 1981a.

PAPAGEORGIOU, A. S. and K. AKI, A specific barrier model for the quantitative description of inhomogeneous faulting and the prediction of strong ground motion II. Applications of the model, Proc. USGS Workshop XVI, 353–404, 1981b.

SATO, T. and T. HIRASAWA, Body wave spectra from propagating shear cracks, *J. Phys. Earth*, **21**, 415–431, 1973.

SENO, T., K. SHIMAZAKI, P. SOMERVILLE, K. SUDO, and T. EGUCHI, Rupture process of the Miyagi-Oki, Japan, earthquake of June 12, 1978, *Phys. Earth Planet. Inter.*, **23**, 39–61, 1980.

SUZUKI, Y. and T. HIRASAWA, Characteristics of source spectra expected from a moving stochastic source model, Abst. Meet. Seismol. Soc. Japan, No. 1, B48, 1983 (in Japanese).

TSUCHIDA, H., E. KURATA, and K. SUDO, Annual report on strong-motion earthquake records in Japanese ports (1968), *Tech. Note Port Harbour Res. Inst.*, No. 98, 1970 a.

TSUCHIDA, H., E. KURATA, and K. SUDO, Annual report on strong-motion earthquake records in Japanese ports (1969), *Tech. Note Port Harbour Res. Inst.*, No. 100, 1970b.

TSUCHIDA, H., E. KURATA, and K. SUDO, Annual report on strong-motion earthquake records in Japanese ports (1970), *Tech. Note Port Harbour Res. Inst.*, No. 116, 1971.

UMEDA, Y., An earthquake source model with a ripple generating core, *J. Phys. Earth*, **29**, 341–370, 1981.

YOKOI, T., K. IRIKURA, and T. OHTA, Cut-off frequency of acceleration spectra, Abst. Meet. Seismol. Soc. Japan, No. 1, B66, 1983 (in Japanese).

YOSHIOKA, N. and K. ABE, Focal mechanism of the Iwate-Oki earthquake of June 12, 1968, *J. Phys. Earth*, **24**, 251–262, 1976.